Properties of hybrid steel fiber reinforced alkali activated slag-fly ash composites

PROPERTIES OF HYBRID STEEL FIBRE REINFORCED ALKALI ACTIVATED SLAG-FLY ASH COMPOSITES

X Gao Q L Yu

R Yu H J H Brouwers

Eindhoven University of Technology

The Netherlands

Wuhan University of Technology

China

ABSTRACT. Alkali activated materials have attracted great attention in recent years due to their excellent mechanical properties, durability, thermal stability; as well as the much lower carbon emission and energy costs compared to Portland cement. However, these also suffers from their relatively low flexural strength and high shrinkage compared to Portland cement system. On the other hand, the application of steel fibre in Portland cement systems has proved its advantages in improving the flexural strength, fracture toughness, impact and the efficiency of reducing the shrinkage behaviour of the brittle matrix. The purpose of this study is to design high performance alkali activated slag-fly ash composites that are modified by steel fibres. Mixtures are designed by applying the modified Andreasen & Andersen particle packing model, in order to achieve a condensed matrix. The influences of the fibre length and dosage, as well as the utilization of hybrid fibres on the workability, compressive strength, flexural strength and drying shrinkage are investigated. Additionally, the reaction products of this blended alkali binder are identified by using Fourier transform infrared spectroscopy.

Keywords: Mix design, Alkali activation, Slag-fly ash blends, Hybrid steel fibre, Shrinkage.

H J H Brouwers is professor of Building Materials in the Department of the Built Environment at Eindhoven University of Technology.

Qingliang Yu is currently working as an assistant professor of Building Materials in the Department of the Built Environment, Eindhoven University of Technology.

Rui Yu is currently working as an assistant professor in the State Key Lab of Silicate Materials for Architectures, Wuhan University of Technology, China.

Xu Gao is currently working as a Ph.D. student in the chair Building Materials in the Department of the Built Environment, Eindhoven University of Technology, the Netherlands. His research interests include the modification, modelling and application of alkali activated materials.

INTRODUCTION

In order to reduce the negative environmental impacts, the utilization of alkali activated materials (AAMs) as a substitute has been extensively studied in recent years. This type of materials usually exhibits excellent performance together with low environmental impacts compared to Portland cement [1, 2]. Recently, growing attention is paid to the blended alkaline system that is prepared by mixing calcium enriched precursors and low calcium ones, due to the modified properties such as setting times, workability, shrinkage, mechanical properties and durability [3, 4]. The reaction products in the blended system are mainly stably coexisting C-(A)-S-H and N-A-S-H type gels [5]; the large amount of available calcium and aluminate affects the original structure of N-A-S-H and C-(A)-S-H gels to some extent [6]. Besides, the influences of key synthesizing factors on reaction kinetics, gel characteristics, mechanical properties and durability issues were also intensively investigated.

However, even though excellent performance can be achieved from the blended alkaline systems, the relatively high drying shrinkage due to the nature of both raw materials and activators is still a remaining issue. Besides, the application of steel fibres in Portland cement systems has proven its advantages in improving the flexural strength, fracture toughness, impact and fatigue resistance; as well as the efficiency of reducing the shrinkage behaviour of the brittle matrix. Besides, steel fibres with different lengths play distinct roles in inhibiting the cracks. Those improved properties may also indicate the potential of using steel fibre in alkali activated systems. Bernal et al. [7] applied steel fibres in waterglass activated slag, the results showed that the flexural strength was largely improved and there was a reduction in compressive strength when increasing the fibre content; also water absorption and permeable porosity were reduced. Aydin et al. [8] used long and short steel fibres with the volume fraction up to 2% in waterglass activated slag-silica fume blends, and they reported that as the fibre content increases, there is a reduction in drying shrinkage; while mixes with a higher fibre content and longer length exhibit higher compressive and flexural strength. However, they present limited mechanism study and performance evaluation regarding the effect of hybrid steel fibre on the blended alkaline system.

The objective of this study is to design a high performance alkali activated slag-fly ash composite that is modified by steel fibres. Mixtures are designed by applying the modified Andreasen & Andersen particle packing model. The influences of fibre length and dosage, as well as the utilization of hybrid fibres on workability, mechanical properties, porosity and drying shrinkage are investigated. Additionally, the reaction products of this blended alkali binder are identified by using Fourier transform infrared spectroscopy (FTIR).

EXPERIMENTS

Materials

The solid precursors used in this study were ground granulated blast furnace slag and Class F fly ash. Their major chemical compositions are shown in Table 1. Limestone powder was used as filler; two types of sand were used as fine aggregates: a micro sand (0-1 mm) and a normal sand (0-2 mm). Besides, two types of straight steel fibres were applied: (1) fibre length of 13 mm with a diameter of 0.2 mm; (2) fibre length of 6 mm with a diameter of 0.16 mm. For the alkaline activators, a mixture of sodium hydroxide (analytical level of 99 wt.%) and a commercial sodium silicate solution (27.69% SiO_2, 8.39% Na_2O and 63.92% H_2O by mass) was used.

Table 1 Major chemical composition of slag and fly ash, wt. %

OXIDES	FLY ASH	SLAG
SiO_2	54.62	30.23
Al_2O_3	24.42	12.58
CaO	4.44	40.51
MgO	1.43	9.05
Fe_2O_3	7.21	0.60
Na_2O	0.73	-
K_2O	1.75	0.43
SO_3	0.46	3.47
LOI	2.80	1.94

Mix Design Methodology

In order to maximize the packing of the granular solid materials, the mixes were designed using the modified Andreasen and Andersen (A&A) model. The applied packing model, works as a target function for the subsequent granular optimization of the individual solid materials.

$$P(D) = \frac{D^q - D_{\min}^q}{D_{\max}^q - D_{\min}^q} \tag{1}$$

where P(D) is a fraction of the total solids materials that are smaller than the particle size D (μm), D_{max} is the maximum particle size (μm), D_{min} is the minimum particle size (μm) and q is the distribution modulus. The distribution modulus (q) in the model is used to determine the proportion between the fine and coarser particles in the mixture. In order to achieve an ideal workability, the value of q is fixed at 0.23 for all mixtures in this study, based on the previous experiences [9]. By using an optimization algorithm based on the Least Squares Method (LSM), the proportions of each individual material in the mix are adjusted until an optimum fit between the composed mix grading curve and the target curve is reached. Therefore, the optimized mixture will possess a compact matrix due to the optimal packing. The particle size distributions of the raw materials, the target curve and the resulting integral grading curve of the mixture is shown in Figure 1. Additionally, the fibre contents up to 1% by volume are added internally in the original system; its effect on the packing is not considered in this case but will be investigated in a future study.

Sample Preparation

The activator used in this study has an equivalent sodium oxide (Na_2O) content of 5% by mass of the binder and an activator modulus of 1.4. The water/powder ratio was kept constant as 0.4 in all mixtures. A slag/fly ash ratio of 80/20 by mass is used in all mixtures. Steel fibre contents up to 1% (by volume) with an interval of 0.25% are applied, and mixes with long/short fibre ratios of 80/20, 60/40, 40/60 and 20/80 are studied. All mortar specimens were prepared in a laboratory mixer; the fresh mortar was then poured into plastic moulds of 40 × 40 × 160 mm^3 and vibrated for 1 min, covered with a plastic film on the top surface for 24 h; finally all specimens were demoulded and cured at a temperature of 20°C and a relative humidity of 95% until their testing age.

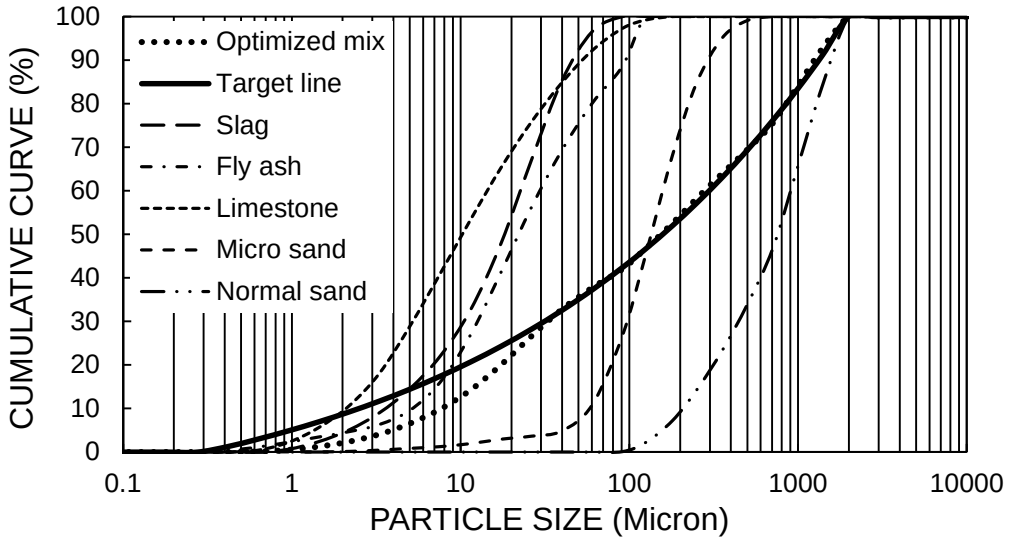

Figure 1 Particle size distributions of the raw materials, the target curve and the resulting integral grading line of the mixture

Testing Methods

The workability of mortar samples was tested by the mini spread-flow test according to EN 1015-3. The compressive strength testing was carried according to EN 196-1. The flexural strength was tested under three-point loading using displacement control. A testing machine controlled by an external displacement transducer was used; the specimen mid-span deflection rate is 0.10 mm/min with a span of 100 mm. FTIR measurements were performed with the wavenumbers ranging from 4000 to 600 cm^{-1} at a resolution of 1 cm^{-1}. The samples for drying shrinkage test were cast in moulds with dimensions of 40 × 40 × 160 mm^3 and cured in sealed condition at a temperature of 20°C. After 24 h of curing, specimens were exposed in a cabinet with a temperature of 20°C and relative humidity of 50%, also the initial length (L_0) was measured at that time. Afterwards, the length (L_n) was measured daily until the age of 28 d.

RESULTS AND DISCUSSION

Flowability

The slump flows of the fresh mortars with fibre additions are depicted in Figure 2. It is shown that as the steel fibre content increases, the slump flow exhibits a gradual decrease in general, and the long steel fibre shows a more significant effect on the slump flow than the short ones. In samples without fibre addition, the slump flow is 25.9 cm; and it slightly decreases to 23.1 cm when the short fibre content increases to 1%. Similar trends are also shown in mixes containing long steel fibres but with a higher decrement when compared to the short fibre. This result is in line with the previous researches that the steel fibre addition presents a negative effect on flowability in both Portland cement system and alkali activated system [10, 11]. It is suggested that the decrease of slump flow is due to the increased surface area and the resulting higher cohesive forces within the matrix. And long steel fibres have a relatively significant influence on this cohesive force. The slump flows of samples with 1% fibre content and different long/short fibre ratios are also tested, those values are all in between of the samples with 1% pure long and short fibres (20.6 and 23.1 cm), following the tendency that a higher long/short fibre ratio exhibits a relatively low slump flow.

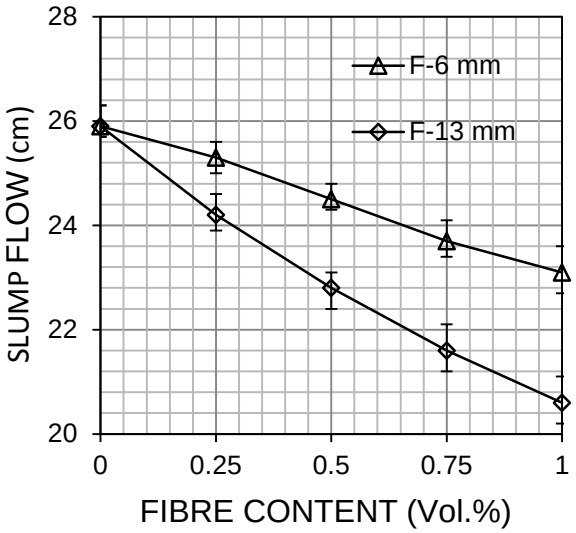

Figure 2 Slump flow of AA slag-fly ash composites with steel fibre addition

Compressive Strength

The 7 and 28 d compressive strengths of mixtures with different long and short fibre contents are presented in Figure 3(a). For the reference sample, the compressive strength is 65.4 MPa at 7 d, and it increases to 81.1 MPa after 28 d of curing. When short fibres with a dosage of 0.25% are added, the compressive strength increases to 71.6 MPa and 85.8 MPa at 7 and 28 d, respectively. It indicates that although steel fibres are well known for improving the tensile or flexural strength, they can also bridge the cracks and retard their propagation to some extent during the compression loads. Further increment of the fibre content from 0.25% to 1% leads to a gradual increase of strength up to 73.35 MPa at 7 d and 89.9 MPa at 28 d, respectively. The mixes with 0.75% and 1% fibre content do not show significant difference in strength, which may reveal that there is a limitation in contributing the compressive strength for steel fibres. The incorporation of long fibres leads to a relatively sharp increase with a dosage of 0.25%, followed by a continuous but slight increase of strength up to around 1%. It is important to notice that mixes with long fibres present higher strengths than the short fibre in general, this is due to the higher efficiency of long steel fibres in inhibiting the growth of macro-cracks.

A total fibre content of 1% is chosen for investigating the effect of hybrid steel fibres. Mixtures with four different long/short fibre ratios (80/20, 60/40, 40/60 and 20/80 vol.%) are applied and the results are presented in Figure 3(b). It can be seen that with a fixed total amount of fibre dosage, the compressive strength firstly increases when lowering the long/short fibre ratio, reaching the maximum strength in mixes with long/short ratio of 60/40, and then followed by a gradual decrease. This result indicates the beneficial effect of using hybrid steel fibre on compressive strength, by doing so a higher strength can be achieved with the same fibre content; and a certain fraction of long/short fibres may exhibit the optimum performance. Additionally, the relatively high strength for all mixes in general is also due to the utilization of particle packing methodology.

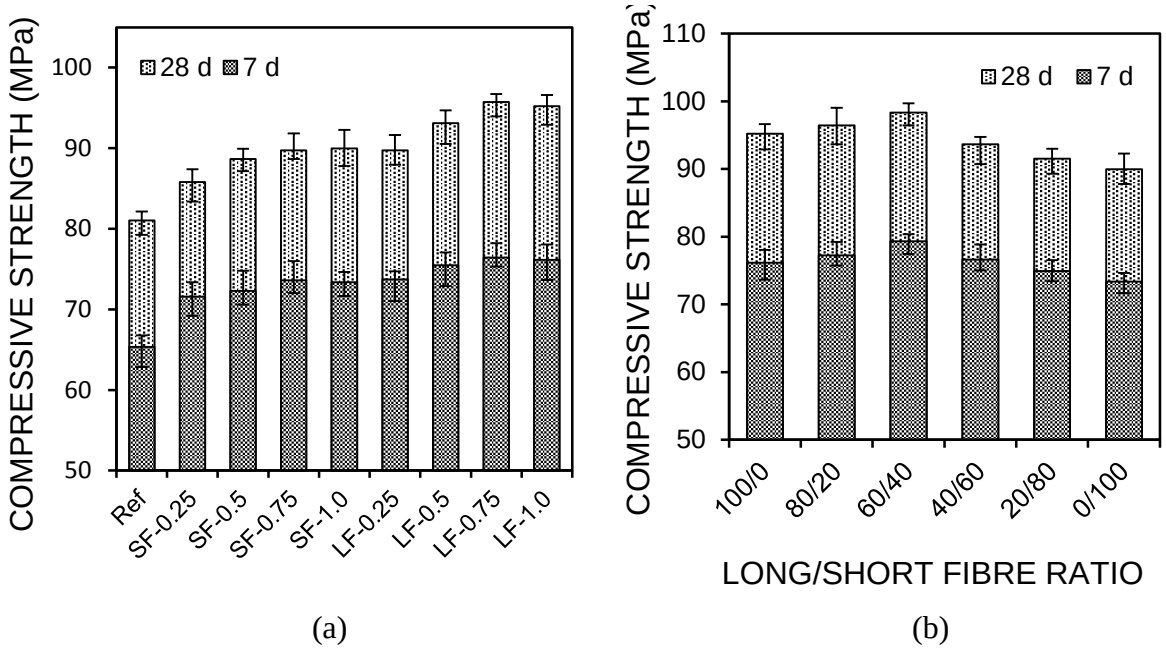

(a) (b)

Figure 3 7 and 28 d compressive strength of AA slag-fly ash composites with fibres (a: single fibre, b: hybrid fibre)

Flexural Strength

The 28 d stress-strain curves of mixtures with long and hybrid steel fibres are shown in Figure 4. The addition of short steel fibres slightly increases the ultimate flexural strength from 8.5 MPa to 11.2 MPa (not shown in the Figure), and the fracture mode of the mixtures with short fibres remains the same as the reference sample: the brittle fracture. This is attributed to shape of this fibre, the relatively short length and diameter makes this fibre capable of inhibiting the micro cracks under flexural loads, thus the flexural strength is increased as a result; while as the loading continues, the micro cracks develop and merge into larger ones and short fibres become less effective in macro crack bridging due to their limited length, and finally brittle fracture occurs. Compared to the effect of short fibres, a more significant increment in ultimate flexural strength and plastic fracture are presented when long fibres were added. The flexural strength continuously increases from 8.5 MPa to 13.5 MPa with the increasing fibre content up to 1%. It can be observed that with the same fibre dosage, mixes with long fibres always present a higher strength, indicating that long fibres are more effective in improving the flexural strength. This is probably due to the longer size of long fibres which makes them more oriented between two imaginary borders, thus a better capacity of preventing the growth of macro cracks can be achieved.

The influence of hybrid steel fibres on flexural strength is presented in Figure 4(b). The fibre content for all mixes is fixed at 1% and samples with only long or short fibres are used as references. As the long fibre fraction increases, mixes show generally a higher energy absorption capacity and a lower stress drop rate after reaching the stress peak; which shows again the higher efficiency of long fibres in bridging the macro-cracks and therefore a more stable post-peak response. The highest flexural strength is shown in mixes with a short/long fibre ratio of 40/60. It confirms that the ultimate flexural strength is not well linked to the toughness; the proportions between the long and short steel fibres exhibit a synergetic effect and result in the occurrence of optimum flexural strength.

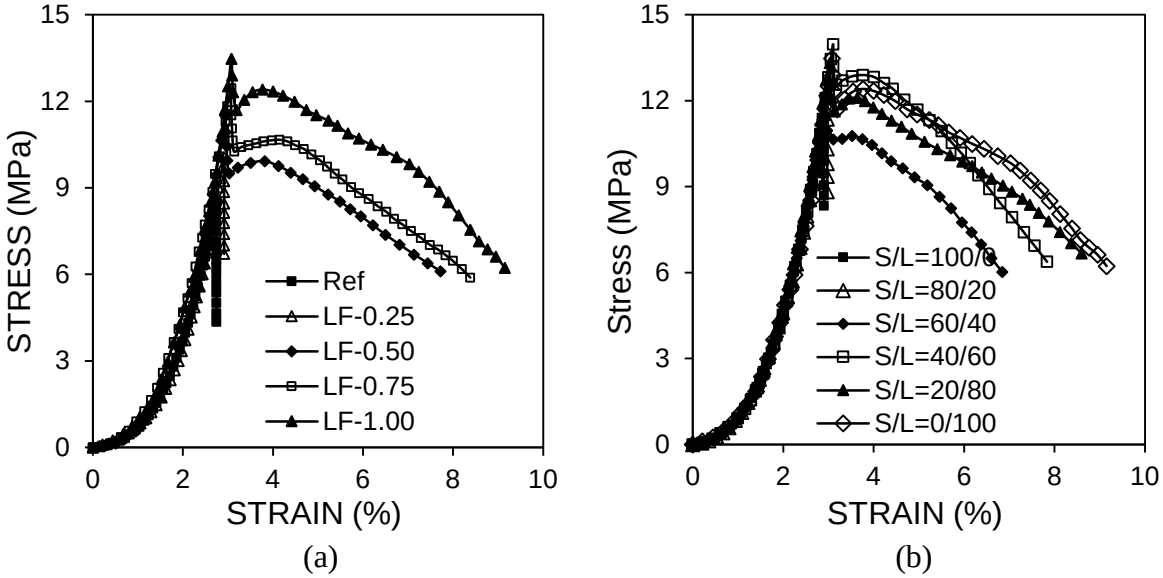

Figure 4 Stress-strain curve of AA slag-fly ash composites with fibre addition (a: long fibre, b: hybrid fibre)

Gel Structure

The infrared spectra of the unreacted slag and fly ash, as well as the reaction products after 1, 7 and 28 d of curing are given in Figure 5. For the starting materials, a main vibration band at around 900 cm^{-1} and a small shoulder at around 670 cm^{-1} are shown in the original slag, which is assigned to the vibration of terminal Si-O bonds and T-O groups [12], respectively. As for the fly ash, a main absorption band at around 1020 cm^{-1}, indicating the presence of large amount of the bridge Si-O-T bonds [13].

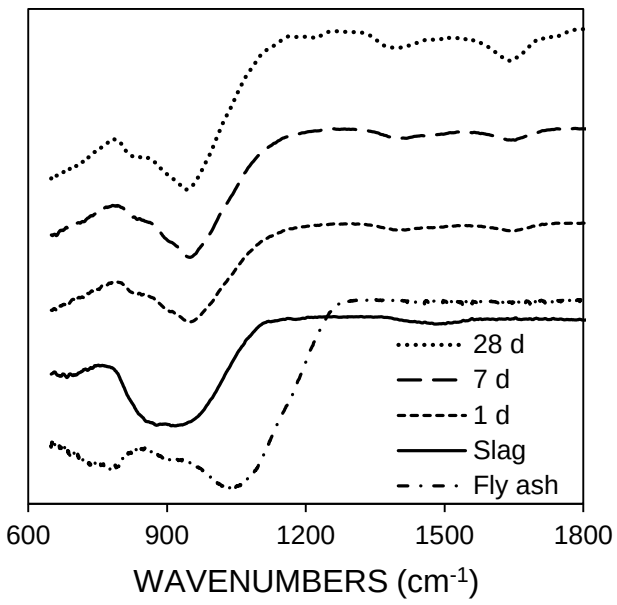

Figure 5 FTIR spectra of the starting materials and AA slag-fly ash blends at 1, 7 and 28 d

After activation, the main absorption band shifts to around 940 cm^{-1} that is assigned to the non-bridging Si-O bonds [14], showing that the main reaction products exhibit a chain structure; and they are generally regarded as C-A-S-H type gels. When compared to the starting materials, the location of the main absorption band shows an increase for slag (from 900 to 940 cm^{-1}) while a decrease for fly ash (from 1020 to 940 cm^{-1}), implying that the original Si-O networks in slag experienced a certain degree of polymerization while the high cross-linked bridging Si-O bonds in fly ash seems to be decomposed to some extent. The slight shoulder at around 815 cm^{-1} together with the absorption band at 1400 cm^{-1} reveal the presence of carbonates, and the absorption bands at 1640 cm^{-1} and around 3200 cm^{-1} (not shown in the figure) are assigned to the vibration of bound water. Concerning the gel structure development, no significant structural changes were observed between the curing age of 1, 7 and 28 d.

Drying Shrinkage

Figure 6 depicts the drying shrinkage results of mixes with only long or short steel fibres until 28 d; each value is an average of two measurements. It is apparent that the reference sample exhibits an obvious length change over time, especially during the first few days, and the addition of both long and short fibre can reduce the drying shrinkage to some extent. It is commonly known that the drying shrinkage is caused by the evaporation of free water from the pores of the hardened matrix [15], and a generally higher drying shrinkage is usually shown in alkali activated materials compared to the Portland cement based materials.

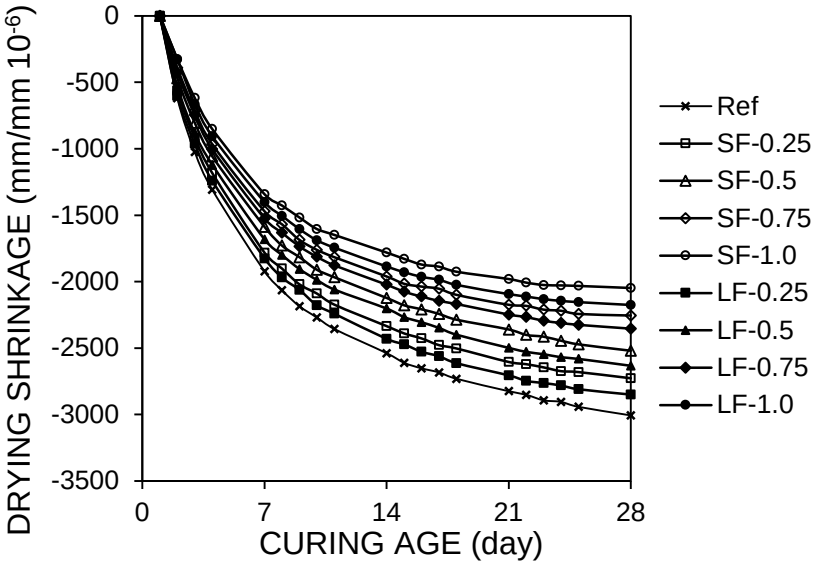

Figure 6 Drying shrinkage of AA slag-fly ash mortars with different fibre lengths

It can be seen that the drying shrinkage decreases with the increasing steel fibre content up to 1%. For a fixed fibre dosage, mixes with long fibre present relatively high values when compared to the ones with short fibre, indicating that the long fibre is slightly less effective than short fibre in inhibiting the shrinkage; but a long fibre addition of 1% still exhibits a shrinkage reduction rate of 27.6% compared to the reference sample. The evaporation of free water from the matrix can result in a reduction of the absolute volume, and meanwhile tensile stresses may arise from the resulted internal restraints. When steel fibre is incorporated, the generated tensile stresses will be imposed on the fibre (on the matrix as well), due to the high elastic modulus and bridging effect of steel fibre, the influence of this inner force on shrinkage

can be suppressed to some extent. The effect of hybrid fibre is not shown in the figure, but the results show that samples with higher short fibre contents exhibit a slightly lower shrinkage, while all mixtures present a similar level of drying shrinkage in general, indicating that the fibre content possesses a more significant influence, and the utilization of hybrid fibre seems not to show any synergetic effect.

CONCLUSIONS

This paper investigates the performance of alkali activated slag-fly ash composites that are reinforced by long and/or short steel fibres, and the mortar samples are designed by applying the modified Andreasen & Andersen particle packing model. The results show that both long and short fibre additions decrease the slump flow, and the utilization of long steel fibres presents a more significant effect. The compressive strength is increased by 10.3%/16.8% when a short/long steel fibre content of 1% is incorporated, respectively. The hybrid usage of long and short fibres presents a synergetic effect and resulting in the presence of an optimum strength. The addition of long fibres with contents higher than 0.25% by volume changes the fracture mode from brittle into plastic; while the addition of short fibres increases the flexural strength moderately. Synergetic effect of long and short fibres is also shown in flexural strength results. The main reaction product of this blended alkali binder is a chain structured C-A-S-H type gel and remains stable after 1 d of curing. The utilization of long and short steel fibres at the dosage of 1% effectively reduces the shrinkage (by 27.6% and 31.9%, respectively) due to their ability of suppressing the generated inner force.

ACKNOWLEDGEMENTS

This research was supported by China Scholarship Council and the Department of the Built Environment at Eindhoven University of Technology. The authors gratefully thank Mr. P. de Vries (ENCI B.V., the Netherlands) and Mr. J. van Eijk (Knauf Insulation, the Netherlands) for the materials supply. Furthermore, the authors wish to express their gratitude to the following sponsors of the Building Materials research group at TU Eindhoven: Rijkswaterstaat Grote Projecten en Onderhoud; Graniet-Import Benelux; Kijlstra Betonmortel; Struyk Verwo; Attero; Enci; Rijkswaterstaat Zee en Delta-District Noord; Van Gansewinkel Minerals; BTE; V.d. Bosch Beton; Selor; GMB; Geochem Research; Icopal; BN International; Eltomation; Knauf Gips; Hess AAC Systems; Kronos; Joma; CRH Europe Sustainable Concrete Centre; Cement & Beton Centrum; Heros and Inashco (in chronological order of joining).

REFERENCES

1. WANG S D, SCRIVENER K L, PRATT P L. Factors affecting the strength of alkali-activated slag, Cem Concr Res, Vol. 24, No. 6, 1994, pp 1033-1043.

2. FERNÁNDEZ-JIMÉNEZ A, GARCÍA-LODEIRO I, PALOMO A. Durable characteristics of alkali activated fly ashes, J Mater Sci, Vol. 42, 2007, pp 3055-3065.

3. LEE N K, LEE H K. Setting and mechanical properties of alkali-activated fly ash/slag concrete manufactured at room temperature, Constr Build Mater, Vol. 47, 2013, pp 1201-1209.

4. SUGAMA T, BROTHERS L E, Van de PUTTE T R. Acid-resistant cements for geothermal wells: sodium silicate activated slag/fly ash blends, Adv Cem Res, Vol. 17, No. 2, 2005, pp 65-75.

5. YIP C K, LUKEY G C, Van DEVENTER J S J. The coexistence of geopolymeric gel and calcium silicate hydrate at the early stage of alkaline activation. Cem Concr Res, Vol. 35, 2005, pp 1688-1697.

6. GARCÍA-LODEIRO I, FERNÁNDEZ-JIMÉNEZ A, BLANCO M T, PALOMO A. FTIR study of the sol-gel synthesis of cementitious gels: C-S-H and N-A-S-H, J Sol-Gel Sci Techn, Vol. 45, 2008, pp 63-72.

7. BERNAL S, GUTIERREZ R D, DELVASTO S, RODRIGUEZ E. Performance of an alkaliactivated slag concrete reinforced with steel fibers, Constr Build Mater, Vol. 24, 2010, pp 208-214.

8. AYDIN S, BARADAN B. The effect of fiber properties on high performance alkali-activated slag/silica fume mortars, Compos Part B: Eng, Vol. 45, 2013, pp 63-69.

9. HÜSKEN G, BROUWERS H J H. Earth-moist concrete: application of a new mix design concept, Cem Concr Res, Vol. 38, pp 1246-1259.

10. RASHAD A M. A comprehensive overview about the influence of different additives on the properties of alkali-activated slag-A guide for Civil Engineer, Constr Build Mater, Vol. 47, 2013, pp 29-55.

11. YU R, SPIESZ P, BROUWERS H J H. Mix design and properties assessment of Ultra-High Performance Fibre Reinforced Concrete (UHPFRC), Cem Concr Res, Vol. 56, 2014, pp 29-39.

12. KOVALCHUK G, FERNÁNDEZ-JIMÉNEZ A, PALOMO A. Alkali-activated fly ash: Effect of thermal curing conditions on mechanical and microstructural development - Part II, Fuel, Vol. 86, 2007, pp 315-322.

13. HAJIMOHAMMADI A, PROVIS J L, Van DEVENTER J S J. Time-resolved and spatially resolved infrared spectroscopic observation of seeded nucleation controlling geopolymers gel formation. J, Colloid Interface Sci, Vol. 357, 2011, pp 384-392.

14. ZHANG Z H, WANG H, PROVIS J L, BULLEN F, REID A, ZHU Y C. Quantitative kinetic and structural analysis of geopolymers. Part 1. The activation of metakaolin with sodium hydroxide, Therm Acta, Vol. 539, 2012, pp 23-33.

15. MA Y W. Microstructure and engineering properties of alkali activated fly ash, PhD Thesis, 2013, Delft University of Technology, Delft, The Netherlands.